Time-Domain Analysis of Open Cavities



Time-Domain Analysis of Open Cavities



Lecture Notes and Computational Exercises* for Graduate Course "Microwave Physics and Applications" Department of Physics, National Tsing Hua University, Hsinchu, Taiwan

The PowerPoint file is based on Prof. K. R. Chu's lecture notes – Time-Domain Analysis of Open Cavities.

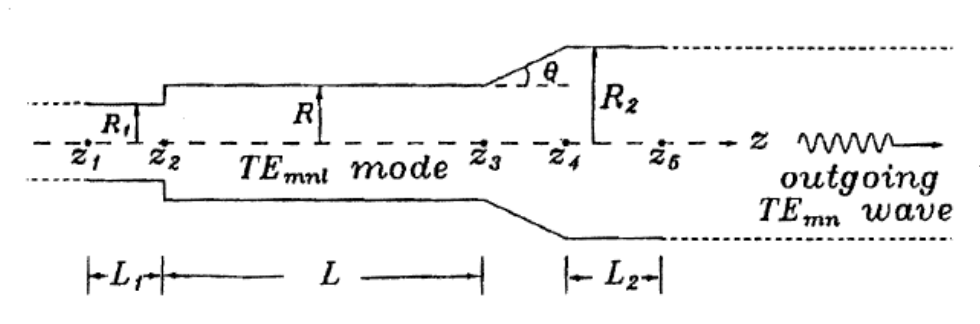




Outline

- 1. Introduction
- 2. Formulation
- 3. Numerical Algorithm
- 4. A Fortran Exercise
- 5. Discussion
- 6. Appendix
- Dispersion relation for a lossy waveguide
- Complex-root finding by Muller's method (Fortran)
- Integration of differential equation using Runge-Kutta (Fortran)
- Spectral domain analysis of open cavity
- Solution to exercise

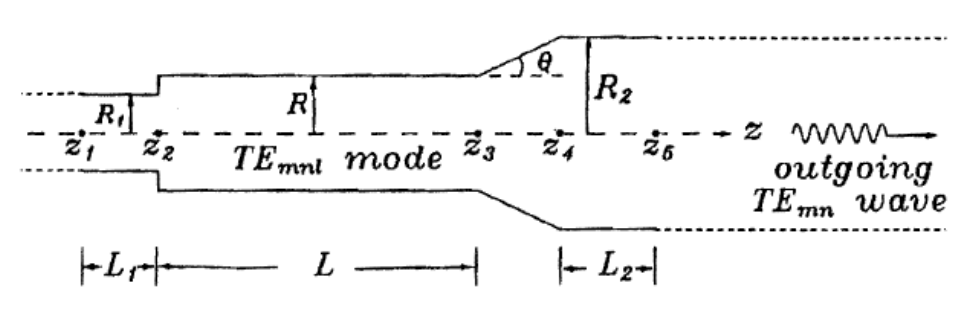
I. Introduction



Caption: Illustrative model of an open cavity. Section $z < z_2$ is a cutoff waveguide (for electron beam entrance). The section between z_2 and z_3 comprises the main body of the cavity. The section between z_3 and z_4 is slightly tapered to provide partial reflection back to the cavity and partial transmission into the output waveguide ($z > z_4$).

- Open cavities are employed in gyrotrons for the generation and extraction of high-power millimeter/terahertz radiation.
- The resonant characteristics depend on the structure. This is a low-Q resonant circuit due to the open-end structure.
- The materials are self-contained and self-explanatory.
- A complementary spectral-domain model can be found in the Appendix.

II. Formulation



Consider a typical open cavity formed of multiple sections of uniform and linearly tapered structures. Find the resonant frequency ω_r and the Q-factor.

3 assumptions:

- The waveguide radius changes slowly, and there is no mode conversion.
- A resonant mode is initially present in the cavity. All fields vary with time as $\exp(-i\omega t)$.
- The end sections are uniform to ensure the correctness of the calculation.

$$\omega = \omega_r + i\omega_i$$
 (where $\omega_i < 0$.)

Time-Domain Analysis

The time dependence of a field component (say B_z) is $B_z \sim e^{-i\omega t} = e^{\omega_i t} e^{-i\omega_r t}$

Field energy
$$\sim |B_z|^2 \sim e^{2\omega_i t}$$
, $(\omega_i < 0)$
Power loss $\sim \left| \frac{d}{dt} \text{ (field energy)} \right| = 2|\omega_i| \cdot \text{ (field energy)}$

Quality factor of the cavity:

$$Q = \frac{\omega_r \text{(field energy)}}{\text{powerloss}} = \frac{\omega_r}{2|\omega_i|}$$

Characteristics of TE_{mn} mode

For a circular waveguide with slowly varying radius $r_w(z)$, the wave equation of TE mode is expressed in a cylindrical coordinate system as,

$$B_z = f(z)J_m[k_{mn}(z)r] e^{im\theta - i\omega t}$$

Applying the boundary condition on the side wall,

$$\frac{\partial}{\partial r} B_z|_{r=r_w(z)} = 0 \implies k_{mn}(z) = \frac{x_{mn}}{r_w(z)},$$

where x_{mn} is the n -th root of $J'_m(x) = 0$

Substituting to the wave equation, we obtain

$$\left[\frac{d^2}{dz^2} + k_z^2(z)\right] f(z) = 0, \text{ where } \begin{cases} k_z^2(z) = \frac{\omega^2}{c^2} - \frac{x_{mn}^2}{r_w^2(z)} & \text{above cutoff} \\ \kappa_z^2(z) = \frac{x_{mn}^2}{r_w^2(z)} - \frac{\omega^2}{c^2} & \text{below cutoff} \end{cases}$$

Field Profile

$$f(z) = \begin{cases} Ae^{ik_z z} + Be^{-ik_z z}, & \text{if } \omega_r > \omega_{cmn} \\ Ce^{\kappa_z z} + De^{-\kappa_z z}, & \text{if } \omega_r < \omega_{cmn} \end{cases}, \text{ where } \omega_{cmn} = \frac{x_{mn}c}{r_w}$$

The complex function of f(z) takes the general form,

$$f(z) = |f(z)|e^{i\Phi(z)}$$

The dependences of f(z) and $\Phi(z)$ on z indicate the nature of the wave.

- For a pure traveling wave (A = 0 or B = 0), |f(z)| is independent of z, but $\Phi(z)$ is a linear function of z.
- For a pure standing wave $(A = \pm B)$, |f(z)| is a sinusoidal function of z.
- For decaying waves at both ends, $\Phi(z)$ is independent of z.

Use the boundary conditions to determine |f(z)| and $\Phi(z)$.

Boundary Conditions

Out-going wave boundary conditions: Initially there is a field profile satisfying all the boundary conditions and then decaying with time.

At both ends, A = D = 0 at $z = z_1$ and C = B = 0 at z_5 .

$$f'(z_1) = \begin{cases} -ik_z(z_1)f(z_1), & \text{if } \omega_r > \omega_{cmn}(z_1) \\ \kappa_z(z_1)f(z_1), & \text{if } \omega_r < \omega_{cmn}(z_1) \end{cases}$$

$$f'(z_5) = \begin{cases} ik_z(z_5)f(z_5), & \text{if } \omega_r > \omega_{cmn}(z_5) \\ -\kappa_z(z_5)f(z_5), & \text{if } \omega_r < \omega_{cmn}(z_5) \end{cases}$$

Numerical Procedure

- With a proper guess of the value of ω_r and $Q(\omega = \omega_r + i\omega_i)$.
- f is given at $z = z_1$ and f' is set accordingly.
- Integrate from z_1 to z_5 using Runge Kutta method
- Check the boundary condition at z_5 and using Muller's method to guess the next root of ω_r and Q.
- Iterative integration, each time with an improved guess for ω , will eventually converge to a correct solution for ω , and f(z) will satisfy all the boundary conditions.

Complex Boundary Condition (cbc sub-rountine)

The boundary condition at $z = z_1$ is given. However, the boundary condition at $z = z_5$ needs to be checked.

$$f'(z_{5}) = \begin{cases} ik_{z}(z_{5})f(z_{5}), & \text{if } \omega_{r} > \omega_{cmn}(z_{5}) \\ -\kappa_{z}(z_{5})f(z_{5}), & \text{if } \omega_{r} < \omega_{cmn}(z_{5}) \end{cases}$$
or
$$D(\omega) = \begin{cases} f'(z_{5}) - ik_{z}(z_{5})f(z_{5}), & \text{if } \omega_{r} > \omega_{cmn}(z_{5}) \\ f'(z_{5}) + \kappa_{z}(z_{5})f(z_{5}), & \text{if } \omega_{r} < \omega_{cmn}(z_{5}) \end{cases}$$

Standard root-finding algorithms such as Muller's method can be readily used.

There are a series of discrete solutions for ω corresponding to different axial modes (assuming that the transverse mode number m and n are given).

Comments

- It is clear that the solution for ω should be independent of the positions of z_1 and z_5 as long as they are in the uniform end sections.
- Validity of the evanescent wave boundary condition requires that the end waveguide radius $(R_1 \text{ or } R_2)$ be smaller than the cavity radius (R).
- It should also be noted that the assumption of slowly varying cross-section is violated at $z = z_2$ (Fig.1). This is justifiable only if the left end waveguide ($z < z_2$) is cutoff to the cavity mode. In this case, total reflection at the left end occurs as a more exact model would predict.

III. Numerical Algorithm How to integrate a differential equation?

$$\left[\frac{d^2}{dz^2} + k_z^2(z)\right] f(z) = 0, \text{ where } \begin{cases} k_z^2(z) = \frac{\omega^2}{c^2} - \frac{x_{mn}^2}{r_w^2(z)} & \text{above cutoff} \\ \kappa_z^2(z) = \frac{x_{mn}^2}{r_w^2(z)} - \frac{\omega^2}{c^2} & \text{below cutoff} \end{cases}$$

The Runge-Kutta method:

The second order equation shown above can be decomposed into the form of coupled real differential equations of the first order.

$$f = f_r + if_i$$

$$f' = f'_r + if'_i$$

$$k_z = k_{zr} + ik_{zi}$$

$$k_z^2 = \operatorname{Re}(k_z^2) + i\operatorname{Im}(k_z^2)$$

$$\Rightarrow \begin{cases} \frac{d}{dz}f_r = f'_r \\ \frac{d}{dz}f_i = f'_i \end{cases}$$

$$\Rightarrow \begin{cases} \frac{d}{dz}f_i = f'_i \\ \frac{d}{dz}f_i' = -\operatorname{Re}(k_z^2)f_r + \operatorname{Im}(k_z^2)f_i \\ \frac{d}{dz}f'_i = -\operatorname{Im}(k_z^2)f_r - \operatorname{Re}(k_z^2)f_i \end{cases}$$

III. Numerical Algorithm Initial Boundary conditions at z₁

The boundary conditions at $z = z_1$ can be written,

$$\begin{cases} f_r(z_1) = \text{arbitrary real constant} \\ f_i(z_1) = \text{arbitrary real constant} \end{cases}$$

$$f'_r(z_1) = \begin{cases} k_{zr}(z_1)f_i(z_1) + k_{zi}(z_1)f_r(z_1), & \text{if } \omega_r > \omega_{cmn}(z_1) \\ \kappa_{zr}(z_1)f_r(z_1) - \kappa_{zi}(z_1)f_i(z_1), & \text{if } \omega_r < \omega_{cmn}(z_1) \end{cases}$$

$$f'_i(z_1) = \begin{cases} -k_{zr}f_r(z_1) + k_{zi}f_i(z_1), & \text{if } \omega_r > \omega_{cmn}(z_1) \\ \kappa_{zi}f_r(z_1) + \kappa_{zr}f_i(z_1), & \text{if } \omega_r < \omega_{cmn}(z_1) \end{cases}$$

III. Numerical Algorithm Final Boundary Conditions at z_5

- A guessed value for ω can now be integrated from z_1 to z_5 .
- The resulting functions $f_r(z_5)$, $f_i(z_5)$, $f_r'(z_5)$ and $f_i'(z_5)$ give $f(z_5)$ and $f'(z_5)$.
- The procedure is to be repeated with an improved guess of until the required accuracy is achieved.

IV. A Fortran Exercise

The program (named CAVITY.f) consists of a main program and the following subprograms.

1. General purpose subprograms.

MULLER: finding the complex roots of an arbitrary complex function (see Appendix B).

RKINT: performing integration of simultaneous differential equations of the first order by the Runge-Kutta method (see Appendix C).

SSCALE and SPLOT (or BSCALE and BPLOT): plotting data conveniently in characters (see Appendix D).

2. Subprograms written for CAVITY (It is recommended to go over the contents closely).

CBC: evaluating the function $D(\omega)$ in Eq. (19) by integrating Eqs. (24)-(27) with initial values given by Eqs. (28)-(31).

DIFEQ: evaluating the derivatives in Eqs. (24)-(27).

RADIUS: specifying the cavity wall radius as a function of z.

RHO: specifying the wall resistivity as a function of z.

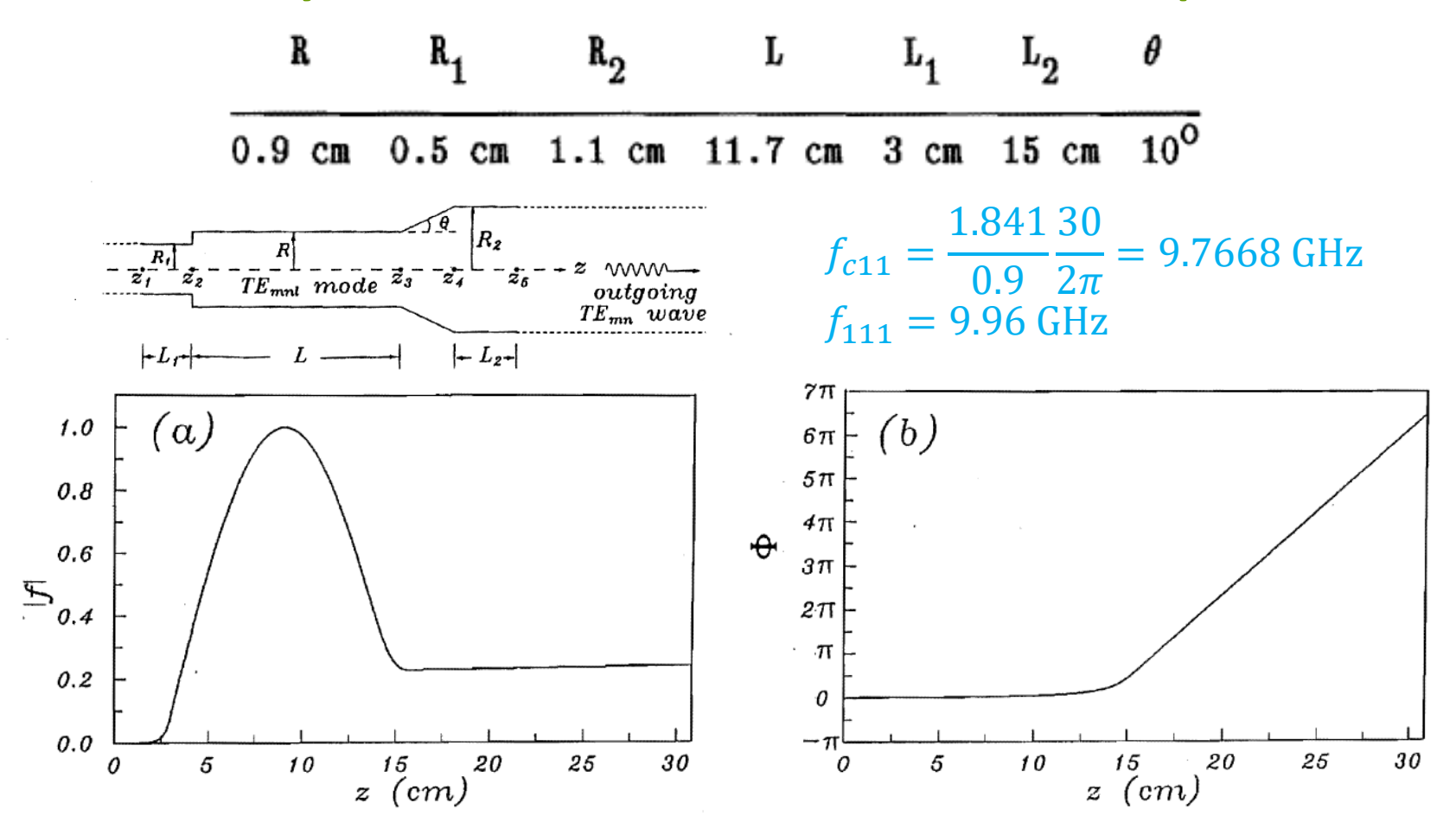
CLOSS: evaluating the wall loss factor derived in Appendix E (The loss factor has been incorporated into the formalism in Appendix F.)

Procedures for Running Program Cavity.f

- To begin with, the cavity dimensions RADIUS, mode of interest, and numerical instructions, etc. are specified in the main program.
- A guessed value of ω is then input into MULLER which calls CBC to evaluate D(ω). Subprogram CBC calls RKINT to perform the integration from z_1 to z_5 . Subsequently, RKINT calls DIFEQ to evaluate the derivatives at every z-step of the integration.
- Finally, MULLER returns the solution for ω to the main program which prints all the information of interest and calls SSCALE and SPOLT (or BSCALE and BPLOT) to plot |f(z)| and $\Phi(z)$.
- Common blocks are extensively employed for information sharing (e.g., the cavity dimensions specified in the main program and the field profile calculated in subprogram CBC) between the main program and subprograms.

Cavity Dimensions and Calculated Results

Cavity dimensions used for numerical example



 TE_{111} mode field profile |f| and phase angle Φ as functions of z for the cavity shown above.

Wall Resistivity and Loss Factor

- Ohmic wall losses have been included in CAVITY through subprograms RHO and CLOSS.
- Formulation of wall loss can be found in Appendix E.
- As a first exercise, we can ignore this effect (hence RHO and CLOSS) by setting the wall resistivity to zero in the main program.
- The TE_{mn} mode dispersion relation for a vacuum filled waveguide,

$$\omega^{2} - k_{z}^{2}c^{2} - \omega_{cmn}^{2} \left[1 - (1+i)\frac{\mu_{c}\delta}{r_{w}} \left(1 + \frac{m^{2}}{x_{mn}^{2} - m^{2}} \frac{\omega^{2}}{\omega_{mn}^{2}} \right) \right] = 0$$

Check the Validity of the Results (Convergence Test)

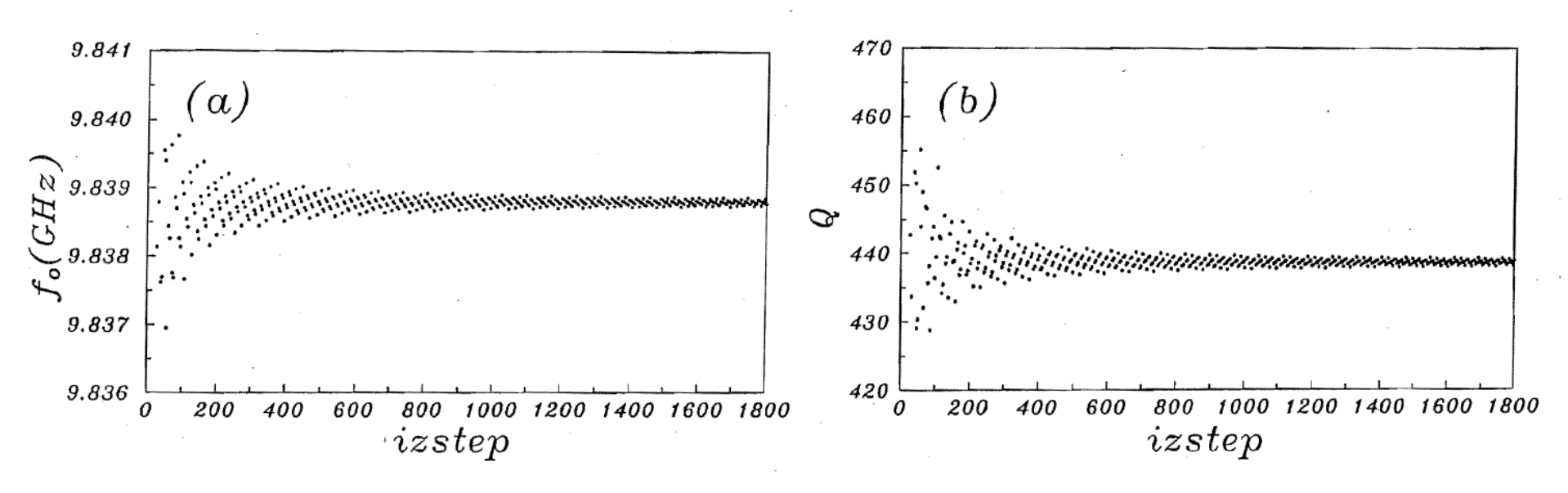
- (i) When calling MULLER to solve for the root of a function (e.g., CF in Appendix B), always monitor the number of times (e.g., ICONT in Appendix B) that the function has been evaluated. For a well-behaved function, the number should be small (less than 10 per root). When the number becomes too large or in the case MULLER is unable to find a root, it is a warning signal of some numerical difficulty due to, for example, erratic behavior of the function (discontinuities and sharp spikes, etc.) or the presence of many closely spaced roots. The result may be in question, or the physics may be unexpected. The warning signal can not be ignored.
- (ii) After MULLER returns a root, always ensure that the resulting function value (e.g., VALUE1 and VALUE2 in Appendix B) is vanishingly small relative to the largest terms of the function. For example, if the function is composed of terms of the order of 10¹⁰, a function value of 10² may be considered vanishingly small (beware of the number of significant digits the computer is capable of handling).

Check the Validity of the Results II

- (iii) A valid root is not necessarily the desired root. For example, we provide a guessed value for the l=2 root and call MULLER to search around it for the correct =2 root. MULLER will return a different root (e.g., l=1 or 3) if the guessed value happens to be a better guess for that root. A reliable way to verify the l number of the root returned by MULLER is to count the number of peaks in |f| versus z.
- (iv) Even with all these checks, there is still no guarantee that the results are free from numerical errors. We must also check whether the step size in the *z*-integration is sufficiently fine to ensure convergence of results.

Check the Validity of the Results III

Figures below show a typical convergence test. The resonant frequency and quality factor Q are plotted as functions of the total number of steps in the z-integration (named IZSTEP in program CAVITY). Note that the positions of the junction points $(z_2, z_3, \text{ and } z_4 \text{ in Fig. 1})$ and hence the cavity dimensions, as resolved on the uniformly spaced axial grid points for the z-integration, are subject to an uncertainty in the magnitude of the step size. This is the primary reason for the fluctuations of and Q with respect to IZSTEP in the approach to convergence. The slow convergence shown in Fig. 4 is predominantly due to the uncertainty of resolving junction point z_2 (where there is a discontinuity in wall radius) on the discrete grid points. Generally speaking, the minimum IZSTEP required for good convergence depends on the circuit geometry and the ratio of the total circuit length to the guide wavelength. Too large an IZSTEP can also bring in accumulation of round-off errors.



Does the Numerical Results Make Sense?

Even computed correctly, numerical results can not be trusted unless they make sense physically. We may start by asking some universal questions: Is the energy conserved (see the slightly positive slope of in Fig. 3a)? Do the results reduce to well known limits [see Exercises (1) below]? Do they exhibit reasonable parametric dependence [see Exercises (2)-(4)]? Do they conform to known scaling laws [see Exercise (5)]? Obtaining answers to these questions is a sure way to become familiar with the problem. We are now ready to go deeper into the problem [see Exercises (6)-(11)] and, for the best reward of all, let our imagination take us to the unexplored territories of research.

Always check carefully!

V. Discussion

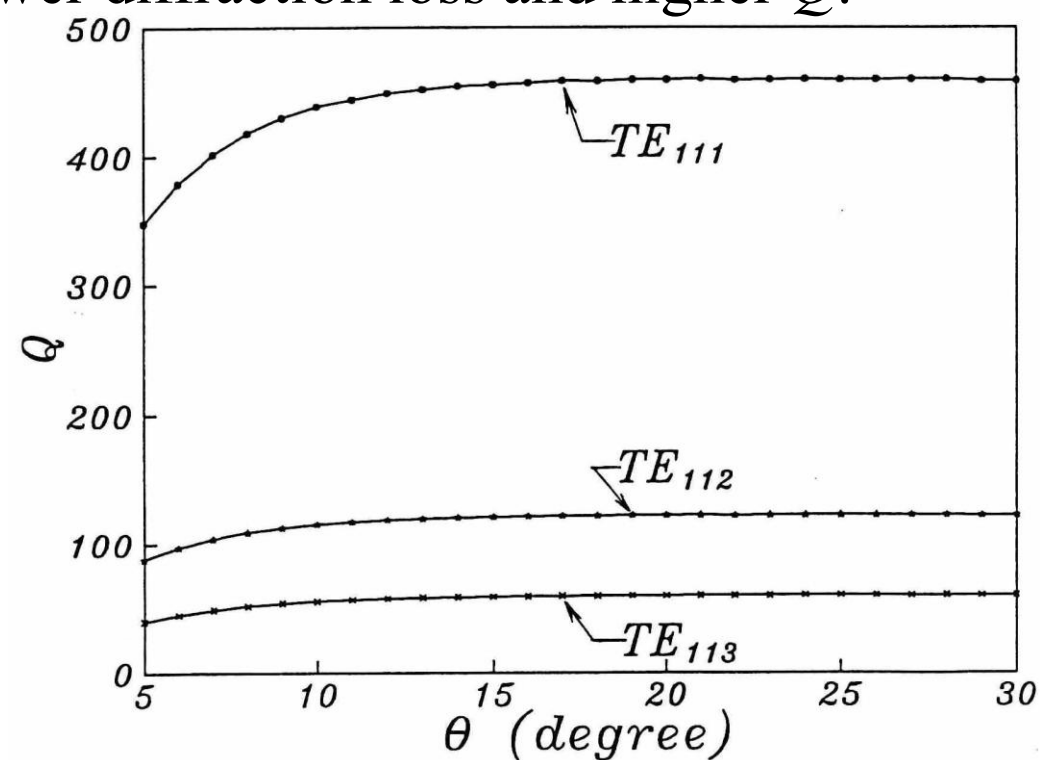
- Computer programs based on the time domain formalism (such as program CAVITY) are extremely effective in that they directly evaluate the resonant frequency, Q, and field profile. They are essential tools for gyrotron designs. Many runs can be rapidly made to achieve the desired resonant frequency and Q, to optimize the field profile and maximize mode separation, etc. However, because of its inability to scan the frequency, the time domain formalism does not present a complete physical picture of the open cavity. The low Q nature of the open cavity brings about some issues that can only be clarified with a spectral domain analysis [see Exercises (8)-(11) and Appendix F].
- Resonances of the type taking place in an open cavity are common in microwave circuits which often contain slightly mismatched junctions between various circuit elements. Single path reflection from one mismatched junction results in a standing wave pattern (measured by VSWR). Multiple reflections between two mismatched junctions result in resonances, much like those of the open cavity. Thus, a circuit with multiple mismatched junctions behaves like coupled open cavities. The resulting circuit resonances are seen on an oscilloscope as multiple spikes superimposed on a swept frequency signal.

1. For the open cavity of Fig. 1 with dimensions given in Table I, the resonant frequency of the TE_{111} mode is 9.839 GHz (see Fig. 4). For an enclosed cylindrical cavity with the same radius (0.9 cm) and length (11.7 cm) as those of the main body of the open cavity, the resonant frequency of the TE_{111} mode is 9.851 GHz. Explain the difference qualitatively.

Sol: Because of the fringe field, the open cavity has an effective length longer than L, hence the resonant frequency (of the $\ell > 0$ modes) is lower than that of an enclosed cavity of length L. It is worth noting that for the $\ell = 0$ (TM) modes of an enclosed cavity for which the axial field profile is uniform, an opening at either end will impose an axial mode structure and therefore increase the resonant frequency.

2. Use program CAVITY to show how the quality factor Q of a given mode varies with the output taper angle θ of the open cavity (keeping other parameters fixed). Interpret the results qualitatively.

Sol: Larger θ results in more reflection from the open end, and hence lower diffraction loss and higher Q.



3. For the cavity dimensions provided in Table I, the quality factors of the first three modes ($\ell = 1, 2, 3$) are, respectively, 439, 116, and 56 (see output data in Appendix A). Give two reasons to explain the rapid drop of Q with the axial mode number.

Sol: Higher ℓ number modes have higher resonant frequencies, which result in (i) less reflection from the open end and (ii) higher group velocity of the wave. Both effects lead to greater diffraction loss through the open end, and hence the decrease in Q values

4. Use program CAVITY to show how the quality factor of a given mode varies with the cavity length L (keeping other parameters fixed). Give three reasons to explain the rapid increase of Q with L.

Sol: A shorter cavity stores less field energy, which further reduces

 $-TE_{111}$

15.0

L(cm)

 TE_{112}

20.0

the Q value. 2000

10.0

8

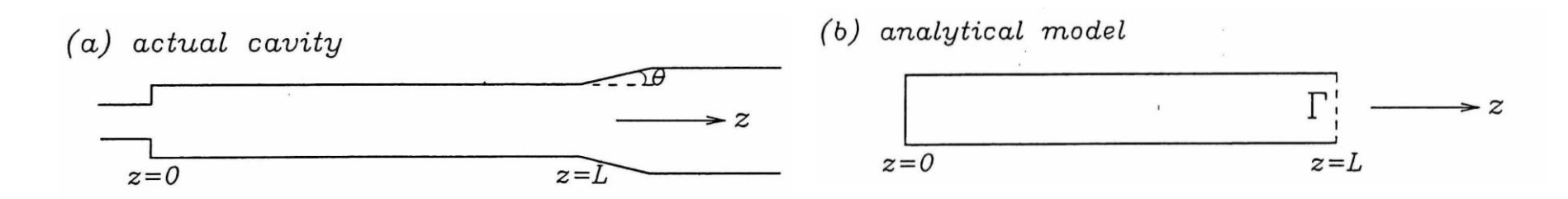
1000

500

5. With reference to Fig. 1, assume that a traveling wave propagating to the left is totally reflected at $z = z_2$ and a traveling wave propagating to the right is partially reflected at $z = z_3$ with a reflection coefficient. Show by the multiple reflection approach (see R.E. Collin, II Foundations for Microwave Engineering", 1st edition, pp. 340-343 and Eq. (49) in Ref. 10 of Appendix F) that the diffraction Q is approximately given by

$$Q \approx \frac{|\Gamma|^{1/2}}{1 - |\Gamma|} \frac{4\pi}{\ell} \left(\frac{L}{\lambda}\right)^2$$

where λ is the free space wavelength of the resonant mode. Compare this relation with the scaling of Q with respect to θ , l, and L as considered in Exercises (2)-(4). Note that it depends on the taper angle and resonant frequency (that is a function of θ and L). If wall losses are included, show that the combined diffractive/ Ohmic Q is given by the above equation with Γ replaced by $\Gamma \exp(-2k_z L)$, where is the attenuation constant which can be evaluated from Eq. (10) of Appendix E.



Exercise 6 and 7

6. Assume that the output waveguide section of the open cavity (see Fig. 1, $z > z_4$) is terminated in a slightly mismatched load. Explain qualitatively how the load will affect the resonant

frequency and Q of the cavity.

7. Use program CAVITY to verify your answer to Exercise (6) by adding a smooth bump on the wall of the output waveguide to simulate the effects of the mismatched load.

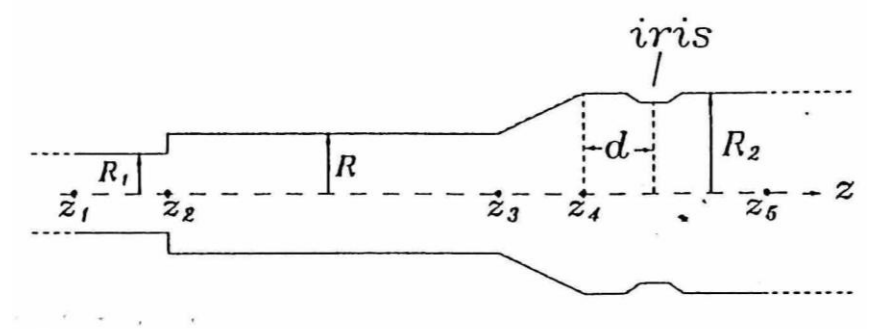
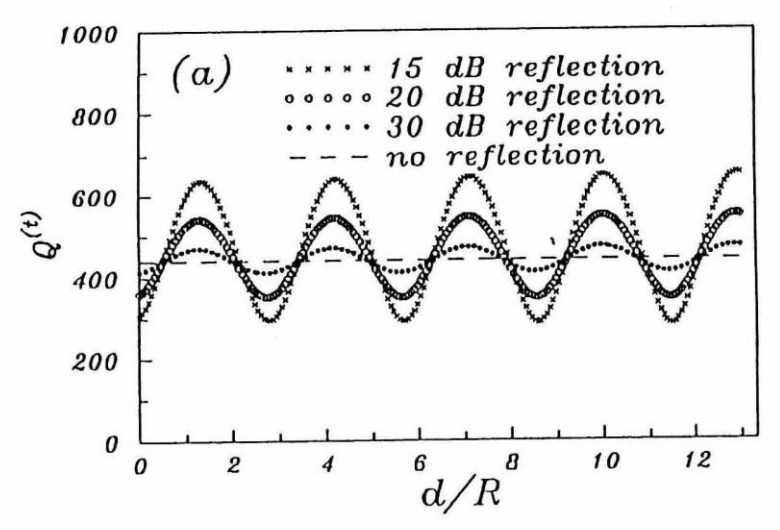
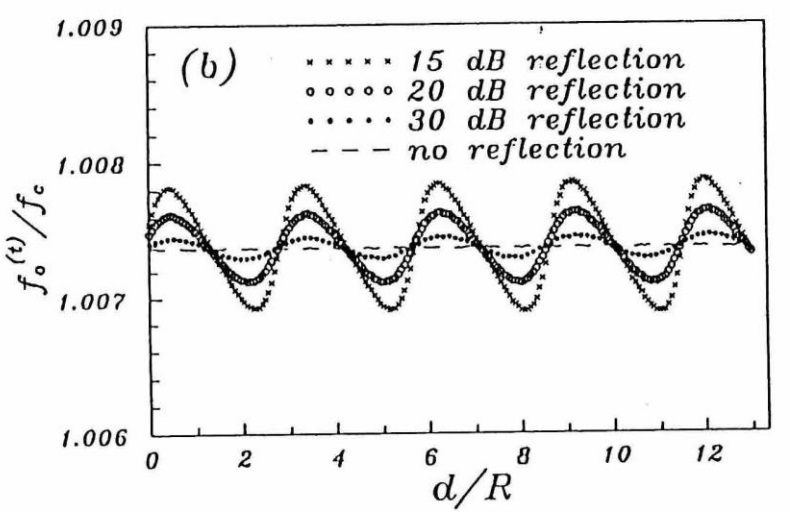
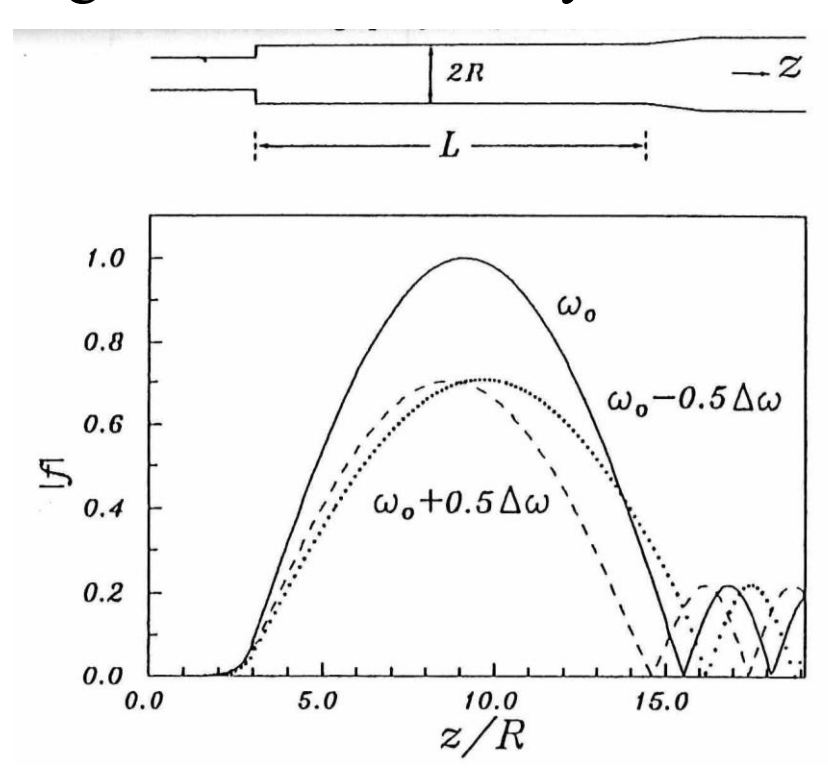


Fig. 9. An iris is added to the output waveguide to model the effects of a mismatched external circuit.



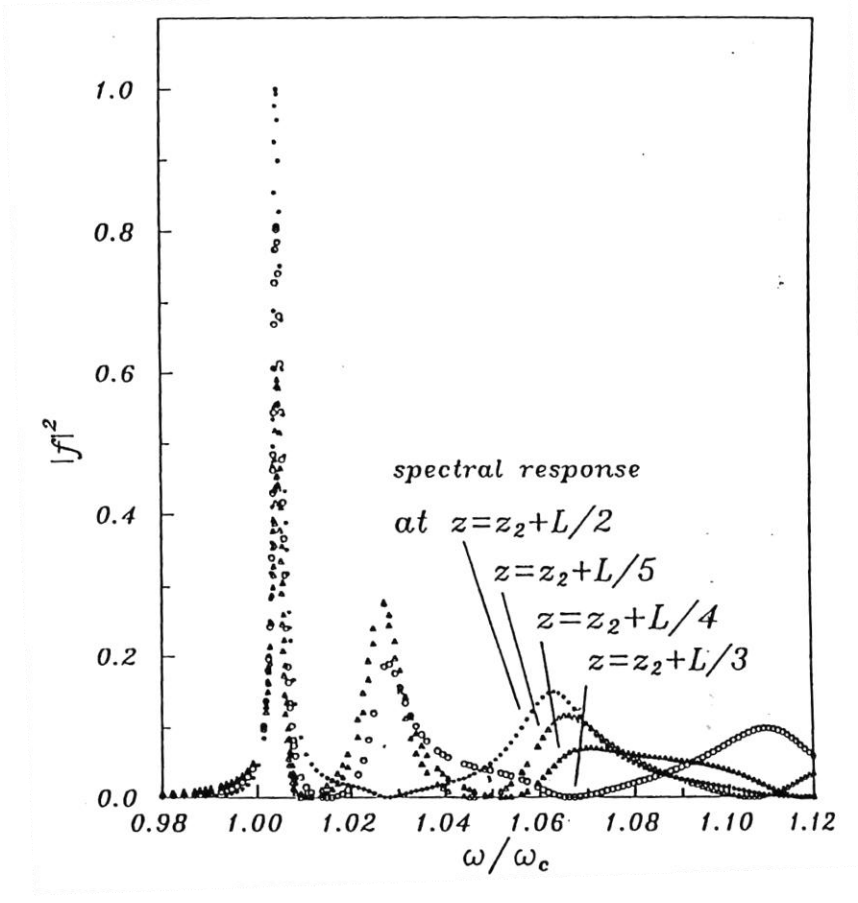


8. The lack of a sharp boundary at the output end of the open cavity is expected to result in a frequency sensitive field profile for a resonant mode, as shown in Fig. 6 of Appendix F. How would the frequency dependent field profile affect the spectral shape of a resonant mode, measured at a <u>fixed</u> position in the cavity, in response to a swept frequency source incident from the output waveguide into the cavity?



9. In Exercise (8), if the fixed-position spectrum is measured at different points along the length of the cavity, will the spectral shape of a given mode be different from point to point? Does this imply that probes located at different axial positions in the cavity will measure different resonant frequencies and *Q*'s for

the same mode?



- 10. Write a computer program based on the spectral domain formalism in Sec. II of Appendix F to:
 - verify your answers to Exercises (8) and (9)
 - calculate the reflection coefficient assumed in Exercise (5) as a function of the wave frequency.
 - calculate the reflection coefficient at the smooth bump assumed in Exercise (7) as a function of the wave frequency.

Sol: RFS or RFS2

11. Program CAVITY calculates Q by its time domain definition (denoted by superscript "t") $Q^{(t)} = \frac{\omega_r}{2|\omega_i|}$

While the spectral domain formalism yields Q by its spectral domain definition (denoted by superscript " ω ") $Q^{(\omega)} = \frac{\omega}{\Delta \omega}$

where $\Delta \omega$ is the FWHM bandwidth. Compare numerical runs made with program CAVITY with those made with the program developed in Exercise (10) to show that, for the same mode of a low Q open cavity, the two definitions of Q do not yield the same result and

Explain this result qualitatively.

$$Q^{(t)} > Q^{(\omega)}$$

$$f(\mathbf{x},t) = \sum_{j} f_{j}(\mathbf{x}) e^{-i\omega_{j}t - \frac{\omega_{j}}{2Q_{j}^{(t)}}t}$$

$$f(\mathbf{x},\omega) = \frac{1}{\sqrt{2\pi}} \int_{0}^{\infty} f(\mathbf{x},t) e^{i\omega t} dt = \frac{1}{\sqrt{2\pi}} \sum_{j} f_{j}(\mathbf{x}) \frac{i}{\omega - \omega_{j} + i \frac{\omega_{j}}{2Q_{j}^{(t)}}}$$

$$|f(\mathbf{x},\omega)|^{2} = \frac{1}{\sqrt{2\pi}} \sum_{j} f_{j}(\mathbf{x}) \frac{i}{\omega - \omega_{j} + i \frac{\omega_{j}}{2Q_{j}^{(t)}}} \frac{1}{\sqrt{2\pi}} \sum_{j} f_{j}^{*}(\mathbf{x}) \frac{-i}{\omega - \omega_{j} - i \frac{\omega_{j}}{2Q_{j}^{(t)}}}$$

$$= \dots \quad \Rightarrow \quad Q^{(t)} > Q^{(\omega)}$$

Appendix: Muller's Method

```
PROGRAM TEST 1 \leftarrow To solve for the roots of f(x)=x^2+1=0
 IMPLICIT REAL (A, B, D-H, J-Ž), COMPLEX (C)
 DIMENSION CROOT (2)
 COMMON ICONT
 EXTERNAL CF
 EP1=1.0E-6
 EP2=EP1
 IMAXIT=50
 ICONT=0 ←—for monitoring the number of times function CF is called by MULLER
 CROOT (1) = CMPLX(0.5, 0.5) \setminus guessed values for roots
 CROOT (2) = CMPLX(0.5, 0.5)
    no. of roots known values of roots (user supplies guessed values, MULLER returns correct values)
                                   accuracy desired
                                                          FALSE.→search for complex roots
 CALL MULLER (0, 2, CROOT, IMAXIT, EP1, EP2, CF, FALSE.) TRUE. -> search for real roots
         no. of roots wanted max. no. of iterations complex functions f(x)
 VALUE1=CABS(CF(CROOT(1)))
 VALUE2=CABS(CF(CROOT(2)))
 WRITE(6,1) CROOT(1), VALUE1, CROOT(2), VALUE2, ICONT
1 FORMAT('ROOT1=',1PE11.4,',',1PE11.4,' (VALUE1=',1PE8.1,')'/
&' ROOT2=',1PE11.4,',',1PE11.4,' (VALUE2=',1PE8.1,')'/
&' ICONT=',I4)
 STOP
 END
 FUNCTION CF (CROOT) \leftarrow--function provided by user to evaluate f(x) when called by MULLER
 IMPLICIT REAL (A, B, D-H, J-Z), COMPLEX (C)
 COMMON ICONT
                                                              Note: Muller's method is discussed in Conte
 CF=CROOT**2+1.0
 ICONT=ICONT+1
                                                              and de boor, Elementary Numerical
 RETURN
 END
                                                              Analysis", (3<sup>rd</sup> edition, Sec. 3.7).
Results returned by MULLER:
                              (cf: analytical solution x=\pm i)
```

ROOT1= 8.3027E-12, 1.0000E+00 (VALUE1= 1.7E-11) ROOT2=-1.9092E-10, -1.0000E+00 (VALUE2= 6.3E-10)

ICONT= 10 ← Total no. of times CF was called to find ROOT1 and ROOT2

Appendix: Runge-Kutta's Method (RKINT)

```
The test program solves for (d^2/dt^2)y = -\sin t for y(t), given y(0) = 0, and (d/dt)y(0) = 1.
    First, we split (d^2/dt^2)y = -\sin t into 2 first order differential equations for
     y_1(t)[\equiv y(t)] and y_2(t)[\equiv (d/dt)y=y'], and let the independent variable t be y_3(t).
     Thus, we have
     (d/dt)y_1 = y_2
                                                      y_1(0) = 0
                                                     y_2(0)=1
     (d/dt)y_2 = -\sin t
                            with intial conditions:
     (d/dt)y_3 = 1
                                                     (y_3(0)=0)
    PROGRAM TEST 2
    IMPLICIT REAL (A,B, D-H, J-Z)
                                             Note: when using RKINT to solve a differential
    DIMENSION Y(90), DY(90), Q(90)
                                                   equation, always check the convergence of results
    EXTERNAL DERIVY
                                                    with respect to the step size (DELT)
    PI=3.1415927
    T0=0.0 \leftarrow initial t
    TF=PI/2.0\leftarrow--final t
    Y(1)=0.0
    Y(2)=1.0
                   initial values of y1, y2 & y3
    Y(3) = T0
    ITMAX=40\leftarrow--no of integration steps between t=0 and t=\pi/2.
    DELT=(TF-T0)/DFLOAT (ITMAX)\leftarrow--step size for t- integration (\Delta t)
    DO 10 I=1, 3
 10 \, Q(I) = 0.0 \leftarrow accuracy indicator (initial values set at 0).
                            user supplies y_1(t), y_2(t),....,RKINT returns y_1(t+\Delta t), y_2(t+\Delta t),....
    DO 100IT=1, ITMAX ↑
                                  ->values of y' returned by RKINT
100 CALL RKINT (DERIVY, Y, DY, Q, 1, 3, DELT)
                                        subroutine provided by user to evaluate y'1, y'2....etc. when called by RKINT.
    PRINT 1, Y(3), Y(1), Y(2)
  1 FORMAT (' T=', 1PE13.6,', Y(1)=',1PE13.6,', Y(2)='1PE13.6)
    STOP
    END
                                                   last equation to be integrated
   SUBROUTINE DERIVY (Y, DY, IEQFST, IEQLST)
   IMPLICIT REAL (A, B, D-H, J-Z) †first equation to be integrated
   DIMENSION Y(1), DY(1)
   DY(1)=Y(2)
   DY(2) = -SIN(Y(3))
   DY(3)=1.0
   RETURN
   END
   Results returned by RKINT at t=\pi/2:
                                                                     cf. analytical solutions
T=1.570797E+00, Y(1)=9.999997E-01, Y(2)=-3.269079E-07
                                                                     y_1(t) \equiv y(t) = \sin t
                                                                     y_2(t) \equiv y'(t) = \cos t
```

at $t=\pi/2$

Spectral-Domain Analysis of Open Cavities

Reason: Cold tests of open cavities almost always employ the method of frequency sweeping, and Q is measured by its spectral domain definition (hence denoted by superscript ω), where $\Delta \omega$ is the full width between the half maxima of the resonant line.

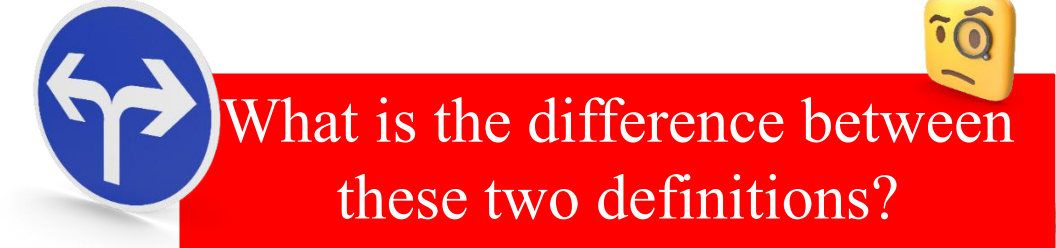
Quality factor of the cavity:

Time-domain definition:

$$Q^{(t)} = \omega_r \frac{\text{field energy}}{\text{powerloss}} = \frac{\omega_r}{2|\omega_i|}$$

Frequency—domain definition:

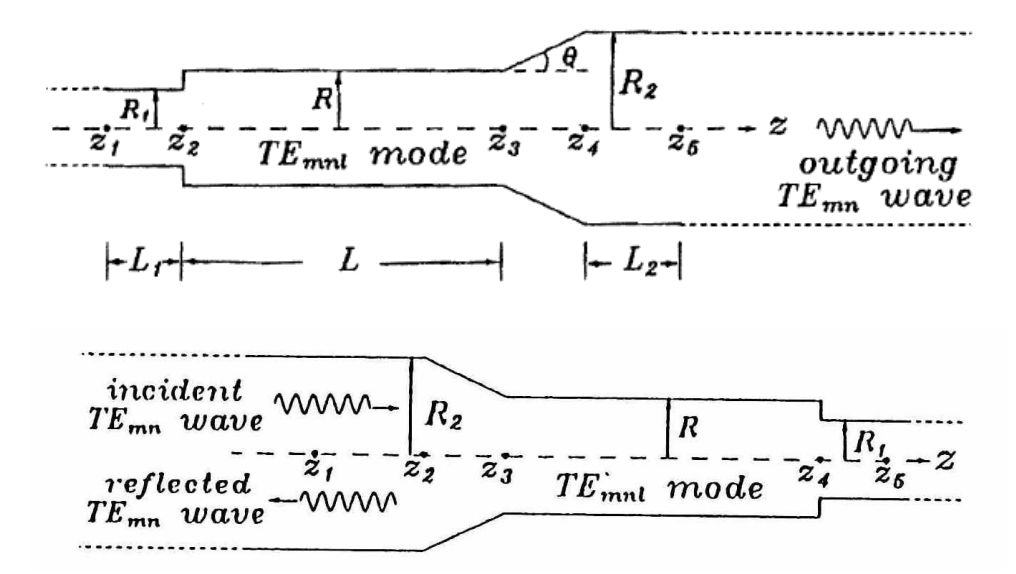
$$Q^{(\omega)} = \frac{\omega_0}{\Delta \omega}$$



II. Numerical Approaches for the Spectral Model

3 assumptions:

- The waveguide radius changes slowly and there is no mode conversion.
- A resonant mode is initially present in the cavity. All fields vary with time as $\exp(-i\omega t)$.
- The end sections are uniform to ensure the correctness of calculation.



Time-domain model:

$$\omega = \omega_r + i\omega_i$$
 (where $\omega_i < 0$.)

Frequency-domain model:

?

Complex reflection coefficient

Numerical Model

• With a proper guess of the value of Γ ($\Gamma = \Gamma_r + i \Gamma_i$).

$$\begin{cases} f(z_1) = e^{ik_z(z_1)z_1} + \Gamma e^{-ik_z(z_1)z_1} \\ f'(z_1) = ik_z(e^{ik_z(z_1)z_1} - \Gamma e^{-ik_z(z_1)z_1}) \end{cases}$$
 where $\omega_r > \omega_{cmn}$

- f is given at $z = z_1$ and f' is set accordingly.
- Integrate from z_1 to z_5 using Runge-Kutta method
- Check the boundary condition at z_5 and use Muller's method to guess the next root of Γ .
- Iterative integration, each time with an improved guess for Γ , will eventually converge to a correct solution for Γ , and f(z) will satisfy all the boundary conditions.

Frequency Response

Table I. Normalized cavity dimensions used for numerical examples (cf. Fig. 1)

L/R	R_1/R	R_2/R	0	
13	0.56	1.22	10 ⁰	

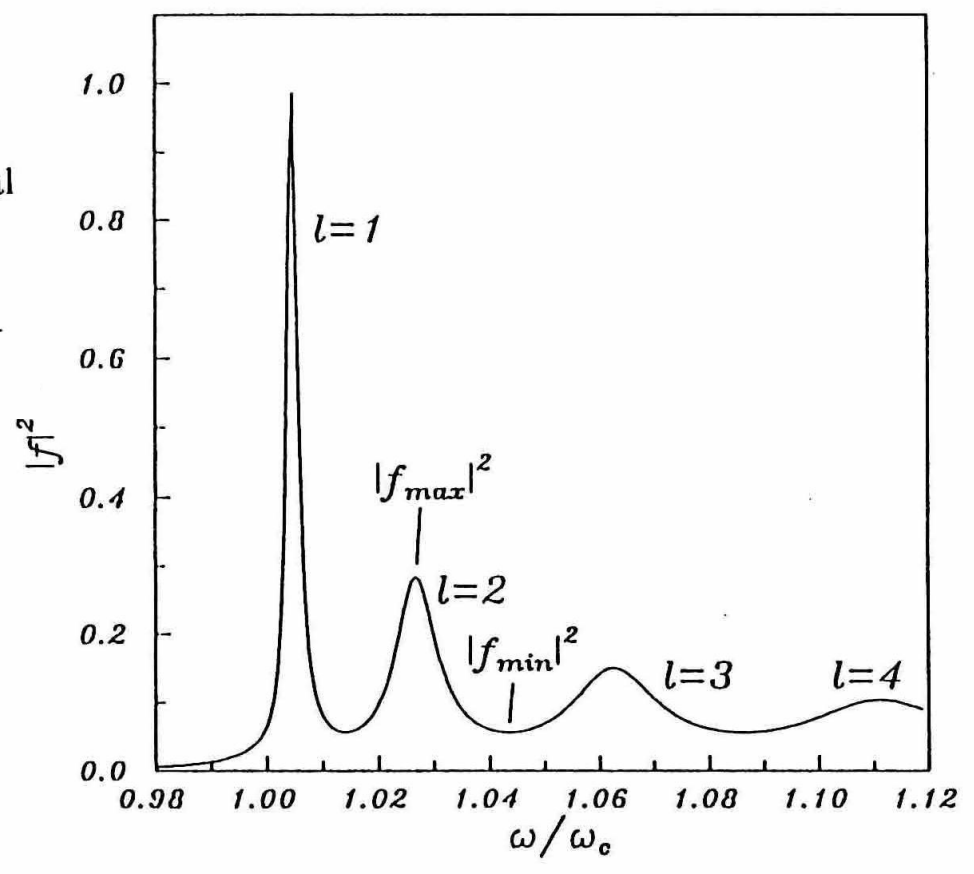


Fig. 3. Caculated maximum—field spectrum of the $TE_{11}^{}\ell$ modes in response to a TE_{11} wave of constant amplitude incident from the output waveguide (see Fig. 2). [f] is the spatial maximum of the field amplitude at a given frequency. $|f_{\text{max}}|$ and $|f_{\text{min}}|$ are, respectively, the spectral maximum and minimum of a given mode. ω_c is the angular cutoff frequency of the main body of the cavity (radius R). Cavity parameters of Table I were used.

Numerical Results

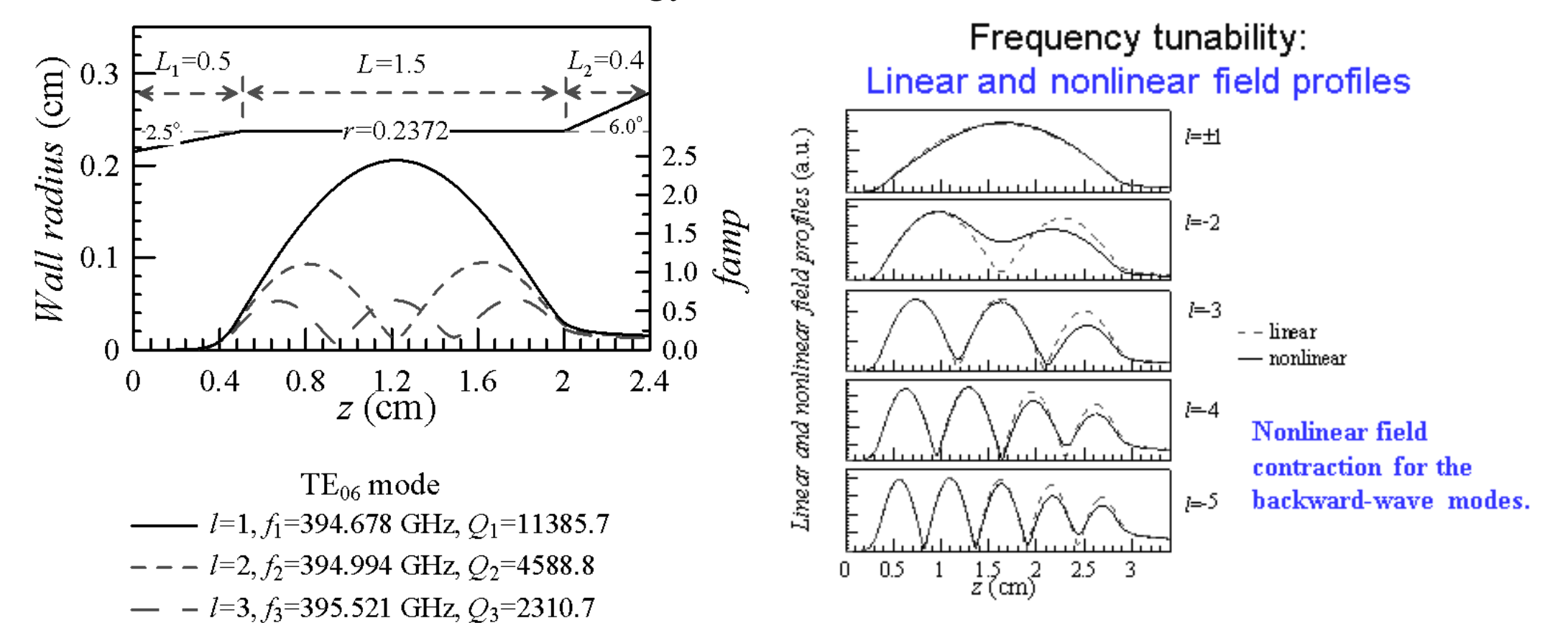
Numerical results obtained under the temporal and spectral models for the cavity dimensions in Table I with different output taper angles θ . TE₁₁₁ were calculated. $f_{\rm c}$ is the cutoff frequency of the main body of the cavity.

θ	l	$\frac{f_0^{(t)}}{f_c}$	$\frac{f_0^{(\omega)}}{f_c}$	Q ^(t)	$Q^{(\omega)}$	$rac{Q^{(t)}}{Q_{ref}}$	$\frac{Q^{(\omega)}}{Q_{ref}}$	$\frac{ f_{min} ^2}{ f_{max} ^2}$
4 ⁰	1	1.0069	1.0069	311.80	298.86	1.6869	1.6166	0.117
4 ⁰	2	1.0275	1.0278	78.66	62.56	0.8173	0.6496	0.372
4 ⁰	3	1.0622	1.0629	36.20		0.5280		0.604
7 ⁰	1	1.0071	1.0072	402.24	390.31	2.1750	2.1102	0.071
7^{0}	2	$1.0\dot{2}83$	1.0286	104.28	92.66	1.0817	0.9607	0.248
7°	3	1.0627	1.0634	48.96	33.91	0.7132	0.4935	0.461
7°	4	1.1093	1.1108	29.38		0.5239		0.648
10°	1	1.0074	1.0074	438.84	430.44	2.3718	2.3262	0.057
10°	2	1.0292	1.0293	115.36	106.08	1.1947	1.0983	0.201
10°	3	1.0646	1.0650	55.44	44.49	0.8048	0.6454	0.378
10°	4	1.1124	1.1130	34.41		0.6102		0.543

Example I

Frequency Tunable Terahertz Gyrotron 394 GHz Using Open Cavity Structure

Novel mechanism: Reflected gyrotron backward-wave oscillator

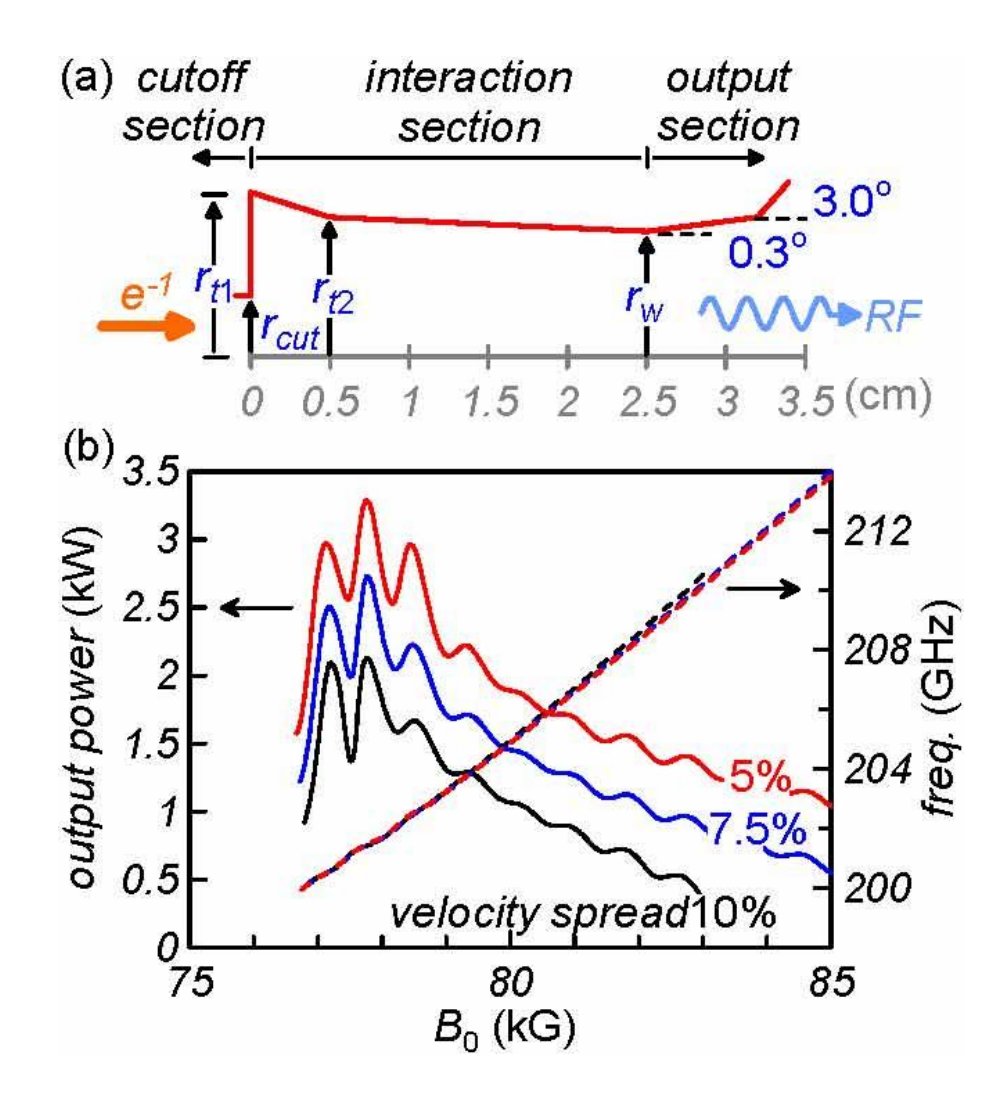


T. H. Chang*, T. Idehara, I. Ogawa, L. Agusu, C. C. Chiu, and S. Kobayashi, "Frequency tunable gyrotron using backward-wave components", J. Appl. Phys. 105, 063304 (2009). Citation: 179

Example II Frequency Tunable Terahertz Gyrotron 203 GHz With Mode Selectivity

An on-going research with Japan Fukui Univ.

N. C. Chen, T. H. Chang*, C. P. Yuan, T. Idehara and I. Ogawa, "Theoretical investigation of a high efficiency and broadband sub-terahertz gyrotron", Appl. Phys. Lett. 96, 161501 (2010). Citation: 49



The End of Open Cavity

